

# Lateral Ordering of InAs Quantum Dots on Cross-hatch Patterned GaInP

Teemu Hakkarainen · Andreas Schramm ·  
Antti Tukiainen · Risto Ahorinta · Lauri Toikkanen ·  
Mircea Guina

Received: 19 June 2010/Accepted: 6 August 2010/Published online: 20 August 2010  
© The Author(s) 2010. This article is published with open access at Springerlink.com

**Abstract** We report the use of partially relaxed tensile as well as compressively strained GaInP layers for lateral ordering of InAs quantum dots with the aid of misfit dislocation networks. The strained layers and the InAs QDs were characterized by means of atomic force microscopy, scanning electron microscopy, and X-ray reciprocal space mapping. The QD-ordering properties of compressive GaInP are found to be very similar with respect to the use of compressive GaInAs, while a significantly stronger ordering of QDs was observed on tensile GaInP. Furthermore, we observed a change of the major type of dislocation in GaInP layers as the growth temperature was modified.

**Keywords** Molecular beam epitaxy · III-V semiconductors · Quantum dots · Ordering · InAs · GaInP

## Introduction

The fabrication of high-quality, coherently strained quantum dots (QDs) is necessary for numerous electronic and photonic applications. Self-assembled QDs obtained from the Stranski–Krastanov (SK) growth mode fulfill the quality requirements for fabrication of devices, such as QD-based laser diodes and detectors. A disadvantage of the self-organizing SK growth is that the QDs are randomly distributed. Ability to create ordered QD structures, i.e. deterministically positioned QDs, is essential for enabling

new optical and electronic applications, such as single-photon emitters, single-electron transistors, or QD-based memory devices. One way to affect the distribution of SK QDs is to exploit the strain sensitivity of the growth process [1, 2], which can be utilized as a tool for ordering the QDs.

The strain field around misfit dislocations (MDs) in a partially relaxed compressively strained (CS) GaInAs layer grown on a GaAs substrate has been shown to be promising in ordering InAs QDs [3–6]. Nevertheless, GaInAs has a relatively low band gap difference with respect to InAs, GaInAs, or InP QDs, while a strong confinement of charge carriers would be desirable in most optical applications. As a solution, we here propose using partially relaxed GaInP layers, which not only have a higher band gap than GaInAs but also enable both compressively (CS) as well as tensile-strained (TS) growth on a GaAs substrate. Non-relaxed GaInP layers grown on GaAs substrates have been successfully used as templates for InP and InAs QDs [7, 8] and as a tool for engineering the properties of InAs QDs [9]. Furthermore, a strong ordering of InP QDs has been observed on partially relaxed CS-GaInP [10]. In this article, we present lateral ordering of InAs QDs on TS- and CS-GaInP layers and compare these two cases with CS-GaInAs. So far, it has been shown that the ordering of QDs can be achieved by exploiting the strain field of a MD [3–6] or surface morphology [11], but here we show that these two effects can be combined together in order to enhance ordering of QDs.

## Experiment

A set of four QD samples was grown on GaAs(100) substrates by solid-source molecular beam epitaxy. All the QD samples were comprised a 60-nm thick partially relaxed, strained layer capped with a GaAs layer and covered with

T. Hakkarainen (✉) · A. Schramm · A. Tukiainen ·  
R. Ahorinta · L. Toikkanen · M. Guina  
Optoelectronics Research Centre, Tampere University of  
Technology, Korkeakoulunkatu 3, 33720 Tampere, Finland  
e-mail: teemu.hakkarinen@tut.fi

InAs QDs. The materials of the strained layers investigated here are CS-Ga<sub>0.85</sub>In<sub>0.15</sub>As (sample A), CS-Ga<sub>0.38</sub>In<sub>0.62</sub>P (samples B and C), and TS-Ga<sub>0.66</sub>In<sub>0.34</sub>P (sample D), all being 1% lattice mismatched to the GaAs substrate, the first two compounds being compressively and the third tensile-strained. The CS-Ga<sub>0.85</sub>In<sub>0.15</sub>As and CS-Ga<sub>0.66</sub>In<sub>0.34</sub>P layers in samples A and B, respectively, were grown at 520°C. The TS-Ga<sub>0.66</sub>In<sub>0.34</sub>P layer in sample D was grown at a lower temperature of 430°C in order to avoid transition from 2D to 3D growth mode, which is typical for this material when grown at higher temperature [12]. For the sake of comparison, we also prepared a QD sample C with a CS-Ga<sub>0.38</sub>In<sub>0.62</sub>P layer grown at 430°C. The strained layers in the QD samples were covered with 30-nm thick GaAs cap layers, which served as templates for 2.2 monolayers (ML) of InAs QDs grown with a growth rate of 0.02 ML/s. The GaAs cap layers and QDs were grown at 540°C. Furthermore, 60- and 80-nm thick TS-Ga<sub>0.66</sub>In<sub>0.34</sub>P layers (samples E and F) without the GaAs cap layer and QDs were grown 430°C in order to determine the critical layer thickness for the formation of dislocations in this TS material. Further details of the samples are listed in Table 1.

For post-growth characterization, we used atomic force microscopy (AFM), scanning electron microscopy (SEM), and high-resolution X-ray diffractometry (HR-XRD). AFM was used for analyzing the surface morphology of the samples as well as for determination of the average heights ( $h_{\text{QD}}$ ) and densities ( $\rho_{\text{QD}}$ ) of the QDs. The lateral ordering of QDs on dislocations was investigated with SEM. HR-XRD reciprocal space maps (RSM) were measured around (004) and (113) reflections for both [011] and [0–11] sample orientations in order to determine the crystal quality, In composition ( $x_{\text{In}}$ ) and relaxation state ( $R_{[\text{hkl}]}$ ) of the strained layers.

## Results and Discussion

Before discussing the lateral ordering of QDs on the MD networks induced by the TS- and CS-GaInP and -GaInAs

layers, it is necessary to evaluate the critical thickness and the type of dislocations generated. The critical thickness for the TS-Ga<sub>0.66</sub>In<sub>0.34</sub>P was estimated based on the SEM observations of the dislocation induced lines on the sample surfaces (not shown) and RSM results. The values of relaxation as well as major dislocation types for each sample are listed in Table 1. According to the RSM measurement, sample E was fully strained and no lines were observed in the SEM pictures. On the other hand, sample F showed a very low density of [0–11]-oriented  $\beta$ -dislocations indicating an early stage of strain relaxation. Thus, the critical thickness of TS-Ga<sub>0.66</sub>In<sub>0.34</sub>P was estimated to be around 80 nm. The critical thicknesses of the CS layers were not determined in this study. However, according to Ref. [4], 50 nm is a sufficient layer thickness to produce a MD network in a Ga<sub>0.85</sub>In<sub>0.15</sub>As layer grown at 520°C. Based on similar surface morphologies (Fig. 3a–c) and values of strain relaxation (Table 1), we assume that CS-Ga<sub>0.38</sub>In<sub>0.62</sub>P and CS-Ga<sub>0.85</sub>In<sub>0.15</sub>As layers investigated here have a critical thickness below 60 nm.

According to Table 1, the major dislocation type in CS-Ga<sub>0.38</sub>In<sub>0.62</sub>P changes from  $\alpha$  to  $\beta$  as the growth temperature is decreased from 520 to 430°C. The thickness of the TS-Ga<sub>0.66</sub>In<sub>0.34</sub>P layer in sample D is lower than the critical value. Hence, the dislocations were actually generated after the GaInP layer growth either during the temperature ramp from 430 to 540°C or during the growth of the GaAs layer. The fact that samples D and F have different major dislocation types suggests that also TS-Ga<sub>0.66</sub>In<sub>0.34</sub>P experiences a change of the major dislocation type as the temperature is increased. What makes this observation interesting is that  $\alpha$ -dislocations have been assumed to be the predominant dislocation type in all cases due to their larger glide velocity [14].

The strain relaxation values on Table 1 show that the strained layers in all of the QD samples are at the early stage of strain relaxation. This is also observed in the RSM of sample D shown in Fig. 1. Both GaAs and GaInP peaks as well as satellite peaks are well observable, indicating good crystal quality and low strain relaxation. The RSMs

**Table 1** Details of the investigated samples.  $x_{\text{In}}$  and  $R_{[\text{hkl}]}$  were calculated from RSM peak data, and  $h_{\text{QD}}$  and  $\rho_{\text{QD}}$  were determined for 1 μm × 1 μm and 10 μm × 10 μm AFM images, respectively [13]. The major dislocation type was determined based on several 20 μm × 20 μm SEM pictures

Sample	Material	Strain	$T_g$ (°C)	$X_{\text{In}}$	$R_{[011]}$ (%)	$R_{[01-1]}$ (%)	$h_{\text{QD}}$ (nm)	$\rho_{\text{QD}}$ (cm <sup>-2</sup> )	Maj. Dislocation type
A	GaInAs	CS	520	0.142	1.60	1.40	13	$5.0 \times 10^9$	$\alpha$ [0–11]
B	GaInP	CS	520	0.618	1.50	1.60	14	$5.1 \times 10^9$	$\alpha$ [0–11]
C	GaInP	CS	430	0.617	1.70	1.60	13	$5.6 \times 10^9$	$\beta$ [011]
D	GaInP	TS	430	0.354	2.60	1.90	16	$4.2 \times 10^9$	$\alpha$ [011]
E	GaInP	TS	430	0.34	0.00	0.00	No QDs	No QDs	No dislocations
F	GaInP	TS	430	–	–	–	No QDs	No QDs	$\beta$ [0–11]

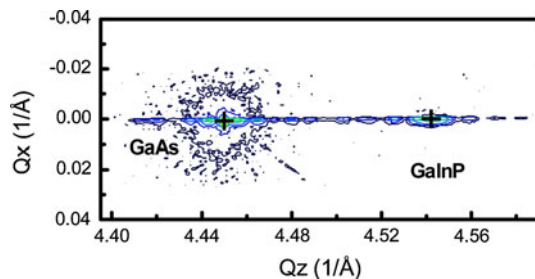


**Fig. 1** XRD reciprocal space map measured from a 60-nm  $\text{Ga}_{0.66}\text{In}_{0.34}\text{P}/\text{GaAs}$  layer (Sample D) around (004) reflection in [011] direction

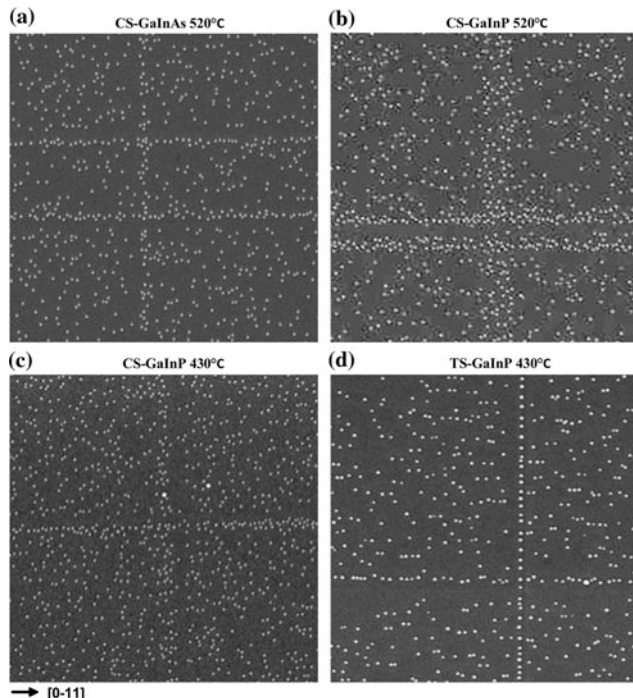


**Fig. 2** SEM pictures ( $3.5 \mu\text{m} \times 3.5 \mu\text{m}$ ) of QD chains on 60-nm partially relaxed GaInP and GaInAs layers. Figures a–d correspond to samples A–D, respectively. The layer material and growth temperature of each sample are indicated in the figure

of the other samples (not presented here) showed similar features.

Figure 2 shows SEM pictures illustrating the ordering of QDs on CS and TS layers. On the CS layers (Fig. 2a–c), the QDs are gathered on MDs, but the ordering is relatively weak. However, on the TS layer (Fig. 2d), the QD accumulation on the MDs differs with respect to the CS layers. On TS layers, the QDs on the MDs are ordered in narrow single-dot wide chains. Furthermore, according to the quantitative data extracted from the AFM pictures and summarized in Table 1, the height and density of the QDs depend on the properties of the strained layer below them; compared to the TS- $\text{Ga}_{0.66}\text{In}_{0.34}\text{P}$ , the QDs on the CS samples are larger and less dense. This can be explained by

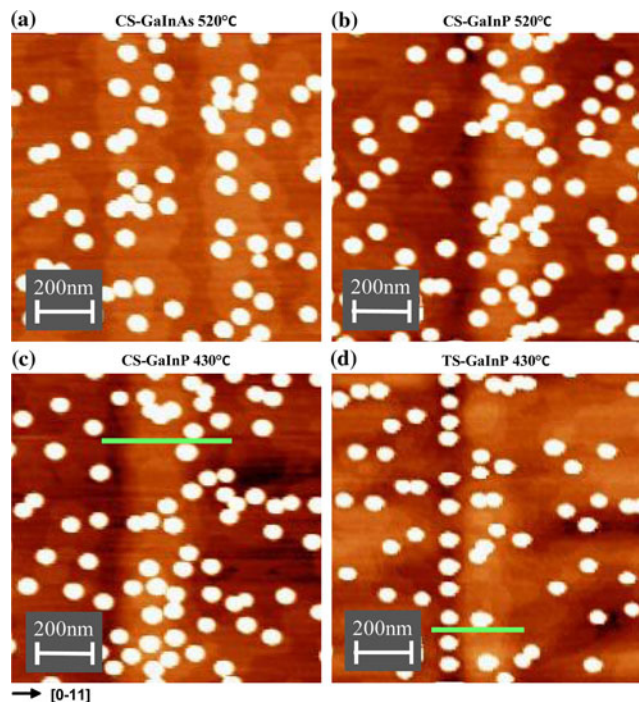


**Fig. 3** AFM pictures of QDs on MDs. Figures a–d correspond to samples A–D, respectively. The color height scale in each image is 5 nm

a reduction of the critical InAs coverage for QD formation due to the compressive strain of the underlying  $\text{Ga}_{0.38}\text{In}_{0.62}\text{P}$  or  $\text{Ga}_{0.85}\text{In}_{0.15}\text{As}$  layer.

In order to interpret the differences of QD accumulations on MDs on TS and CS layers, we analyzed the surface morphology around the QD chains by AFM. The AFM images in Fig. 3, show a clear difference between compressive and tensile strain; the QDs on CS layers are gathered on ridges (Fig. 3a–c), which is consistent with Ref. [2] and [10], while on the TS- $\text{Ga}_{0.66}\text{In}_{0.34}\text{P}$  (Fig. 3d) the narrow QD chains are formed in grooves.

We try to explain the observed differences in ordering by calculating the stress field on the film surface above a MD for both CS and TS layers. The magnitude of the Burgers vector of a mixed  $60^\circ$  MD is  $b = \|b\| = a/\sqrt{2}$ , where  $a$  is the lattice constant [15]. The edge component of  $\mathbf{b}$  can be decomposed into parts parallel and perpendicular to the layer/substrate interface:  $b_{\text{edge}} = b_{\parallel} + b_{\perp}$ . The magnitudes of the in-plane and out-of-plane components of the Burgers vector are

$$b_{\parallel} = \|b_{\parallel}\| = \frac{b}{2}, \quad (1a)$$

$$b_{\perp} = \|b_{\perp}\| = \frac{b}{\sqrt{2}}. \quad (1b)$$

The formation of MDs at the layer/substrate interface induces a local stress field that affects the QD nucleation at

the sample surface. The tangential stress component of pure edge dislocation lying at the distance  $h$  below the surface is

$$\sigma_{xx}^{MD} = \frac{4G}{\pi(1-\nu)} \times \frac{hx(hb_{\perp} - xb_{||})}{(x^2 + h^2)^2}, \quad (2)$$

in which  $G$  is the shear modulus,  $\nu$  is the Poisson's ratio, and  $x$  is the lateral distance from the MD. Figure 4 shows strain profiles calculated with Eq. (2) for a MD in TS and CS layers using values for  $G$  and  $\nu$  indicated in Table 2 and a layer thickness  $h$  of 90 nm. The in-plane and out-of-plane components of the Burgers vector were assumed to be  $b_{||} = -b/2$ ,  $b_{\perp} = -b/\sqrt{2}$  for the CS layers and  $b_{||} = b/2$ ,  $b_{\perp} = -b/\sqrt{2}$  for the TS layer.

In both the CS (Fig. 4a) and the TS layer (Fig. 4b), positive and negative maxima of the stress are formed on the adjacent sides of the MD. This local strain fluctuation affects the growth of the strained layer and GaAs capping

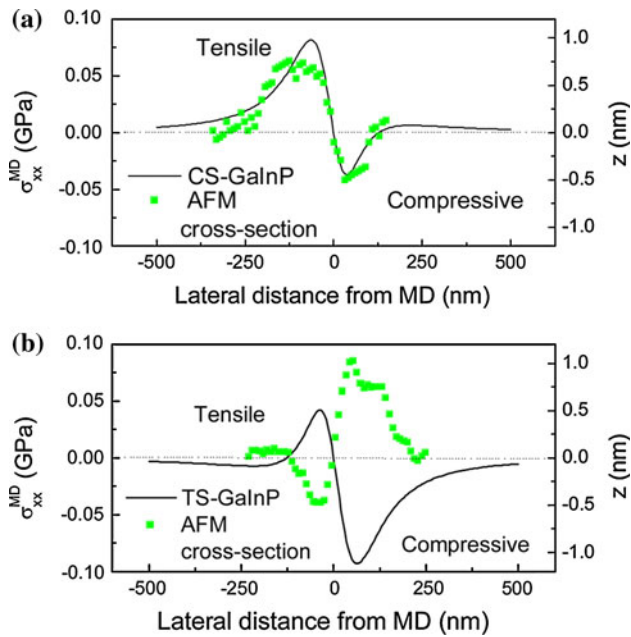


**Fig. 4** Tangential stress component above a misfit dislocation calculated for **a** CS-GaInP and **b** for TS-GaInP layers. The AFM cross-sections in (a) and (b) are measured along the lines in Fig. 3c and d, respectively

**Table 2** Elastic properties of TS-GaInP and CS-GaInP. Elastic constants  $C_{11}$  and  $C_{12}$  are calculated with Vegard's law using values from Ref. [16] for binary compounds. The Poisson's ratio is  $\nu = C_{12}/(C_{11} + C_{12})$ , and the Shear modulus is  $G = (C_{11} - C_{12})/2$

Material	$x_{In}$	$C_{11}$ (GPa)	$C_{12}$ (GPa)	$\nu$	$G$ (GPa)
TS-GaInP	0.34	127.1	60	0.321	33.55
CS-GaInP	0.62	116.1	58.4	0.335	28.86

layer. In Ref. [2], the authors suggested that the surface corrugation above a MD in an un-capped CS-GaInAs layer is caused by formation of In-rich alloy on the tensile part of the stress field of the MD (Fig. 4a). The growth of InAs QDs is also favored in this area of the MD due to their larger lattice constant; hence, the QDs are accumulated on the ridge. The growth of a GaAs cap may also affect the surface morphology. GaAs will most probably avoid the In-rich ridge, which experiences local tensile stress [2] and favor the Ga-rich grooves. The correlation between the stress field of a MD and surface profile for a CS-GaInP is shown in Fig. 4a. It appears that after growth of the GaAs cap the surface corrugation is formed by a ridge and a groove located above the tensile and compressive sides of the MD, respectively. In sample D, the surface corrugation is formed solely during the GaAs layer growth because the MDs are formed after the growth of the strained layer. The compressive stress of a MD locally compensates the tensile strain of the GaInP layer on the right side of the dislocation (Fig. 4b). Therefore, this area is favored by GaAs and a ridge is formed. Correspondingly, GaAs tends to avoid the tensile side of the MD, which becomes a groove. Thus, the groove is formed above the tensile side of the dislocation (Fig. 4b), not above the compressive side as in the CS-GaInP layer. The InAs QDs, however, accumulate on the tensile part of the dislocation. Thus, the ordering of QDs on TS-GaInP is guided not only by the strain field of the dislocation but also by the shape of the groove, while on the CS-GaInP and CS-GaInAs layers, the QDs accumulate on the ridges solely due to stress field of the MDs.

## Conclusions

It was shown that misfit dislocation networks obtained from partially relaxed CS- and TS-GaInP layers can be utilized for lateral ordering of InAs QDs. The strongest QD ordering was observed on TS-GaInP, because of the accumulation of QDs on narrow grooves that are formed during the growth of the GaAs cap layer. The MDs on CS-GaInP and CS-GaInAs layers, in which QDs are mainly gathered on ridges, were shown to have similar QD ordering properties including line distribution and direction as well as QD height and density. Concluding, GaInP is a good candidate for replacing GaInAs in order to align QDs on MD networks and when a material of a higher band gap is required.

**Acknowledgments** We acknowledge financial support from Finnish National Graduate School in Materials Physics, Academy of Finland project DAUNTLLESS (decision number 123951) Jenny and Antti Wihuri Foundation, and Finnish Foundation for Technology Promotion.

**Open Access** This article is distributed under the terms of the Creative Commons Attribution Noncommercial License which permits any noncommercial use, distribution, and reproduction in any medium, provided the original author(s) and source are credited.

## References

1. J. Tersoff, C. Teichert, M.G. Lagally, Phys. Rev. Lett. **76**, 1675 (1996)
2. K. Yamaguchi, E. Waki, H. Hasegawa, Jpn. J. Appl. Phys. **36**, L871 (1997)
3. C.L. Zhang, Z.G. Wang, F.A. Zhao, B. Xu, P. Jin, J. Cryst. Growth **265**, 60 (2004)
4. C.L. Zhang, B. Xu, Z.G. Wang, P. Jin, F.A. Zhao, Physica E **25**, 592 (2005)
5. Chunling Zhang, Lei Tang, Yuanli Wang, Zhanguo Wang, Bo Xu, Physica E **33**, 130 (2006)
6. K. Yamaguchi, K. Kawaguchi, T. Kanto, Jpn. J. Appl. Phys. **41**, 996 (2002)
7. H.N. Carlsson, W. Seifert, A. Petersson, P. Castrillo, M.E. Pistol, L. Samuelson, Appl. Phys. Lett. **65**, 3093 (1994)
8. H. Amanai, S. Nagao, H. Sakaki, J. Cryst. Growth **227**, 1089 (2001)
9. T. Sengoku, R. Suzuki, K. Nemoto, S. Tanabe, F. Koyama, T. Miyamoto, Jpn. J. Appl. Phys. **48**, 070203 (2009)
10. K. Häusler, K. Eberl, F. Noll, A. Trampert, Phys. Rev. B **54**, 4913 (1996)
11. H. Heidemeyer, C. Müller, O.G. Schmidt, Physica E **23**, 237 (2004)
12. X. Wallart, O. Schuler, D. Deresmes, F. Mollot, Appl. Phys. Lett. **76**, 2080 (2000)
13. I. Horcas, R. Fernandez, J.M. Gomez-Rodriguez, J. Colchero, J. Gomez-Herrero, A.M. Baro, Rev. Sci. Instrum. **78**, 013705 (2007)
14. M.J. Matragrano, D.G. Ast, J.R. Shealy, V. Krishnamoorthy, J. Appl. Phys. **79**, 8371 (1996)
15. A.M. Andrews, R. LeSar, M.A. Kerner, J.S. Speck, A.E. Romanov, A.L. Kolesnikova, M. Bobeth, W. Pompe, J. Appl. Phys. **95**, 6032 (2004)
16. I. Vurgaftman, J.R. Meyer, L.R. Ram-Mohan, J. Appl. Phys. **89**, 5815 (2001)